Microchimica Acta (2021) 188: 353
https://doi.org/10.1007/s00604-021-04962-3

ORIGINAL PAPER

Electrochemiluminescence biosensor based on molybdenum disulfide-graphene quantum dots nanocomposites and DNA walker signal amplification for DNA detection

Yina Sun[1] · Chuan Huang[1] · Xiujin Sun[2] · Qian Wang[1,3] · Peini Zhao[3] · Shenguang Ge[1] · Jinghua Yu[3]

Received: 20 May 2021 / Accepted: 26 July 2021 / Published online: 26 September 2021

Abstract

Based on the prominent electrochemiluminescence (ECL) performances of molybdenum disulfide-graphene quantum dots (MoS_2-GQDs) nanocomposite and combined with enzyme-assisted recycling DNA walker signal amplification, an "on-off" switch ECL biosensor was proposed for sensitive assay of specific DNA sequences. Noticeably, MoS_2 with two-dimensional nanosheet structure increased the loading capacity of GQDs to support abundant hairpin DNA (H). The composites of MoS_2 and GQDs facilitated the charge transfer in ECL process, which significantly improved the ECL signal to achieve an "on" state. Then, the DNA walker cyclic amplification was performed by adding the target DNA and exonuclease III (Exo III). Finally, the DNA2-Fc-DNA1 was introduced into the system as ECL signal quencher, turning the ECL signal into an "off" state. The sensitive assay of ultra-low concentration specific DNA sequences was realized according to the variation of ECL signal strength before and after the existence of target DNA. The proposed ECL biosensor showed a good linear relationship ranging from 1 nM to 100 aM with a detection limit of 25.1 aM, providing a powerful strategy for biomedical research and clinical analysis.

Keywords Electrochemiluminescence biosensors · Molybdenum disulfide-graphene quantum dots · DNA walker · Signal amplification

Introduction

The simple, rapid, and ultrasensitive assay of trace specific DNA sequences has significant importance in many areas, for instance, disease diagnosis, biomedical applications, and environmental monitoring [1]. At present, various detection techniques including fluorescence [2], electrochemistry [3, 4], chemiluminescence [5], and electrochemiluminescence (ECL) [6] have been applied to the assay of DNA. Significantly, electrochemiluminescence has brought about the widespread attention owing to its high sensitivity, perfect selectivity, easy controllability, low cost, and broad detection range, providing a promising strategy for specific DNA sequences assay [7, 8]. To further boost the sensitivity of electrochemiluminescence biosensors and achieve the assay of trace DNA, a series of amplification strategies have been proposed, including polymerase chain reaction (PCR) [9], strand displacement amplification (SDA) [10], rolling circle amplification (RCA) [11, 12], and hybridization chain reaction (HCR) [13]. However, these methods still have some limitations, such as strict reaction conditions, high background signal, and false positive signal [14]. DNA walker is a nanomolecular device made of highly programmable DNA self-assembly [15], with the characteristics of high flexibility, prominent sensitivity, and strong specificity, which provides a new way for DNA signal amplification strategy. Pierce et al.

✉ Peini Zhao
zhaopn_1985@163.com

✉ Shenguang Ge
chm_gesg@163.com

[1] Collaborative Innovation Center of Technology, Equipment for Biological Diagnosis, Therapy in Universities of Shandong, University of Jinan, Jinan 250022, People's Republic of China

[2] Shandong Branch of China National Geological Exploration Center of Building Materials Industry, Jinan 250014, People's Republic of China

[3] School of Chemistry and Chemical Engineering, University of Jinan, Jinan 250022, People's Republic of China

demonstrated a four-step DNA walking machine that shifted by moving the hind foot forward to the leading position at each pace, with which the real-time monitoring for walker movement was realized by multiplexed fluorescence quenching [16]. Wang et al. combined the enzymatic recycling cleavage strategy and the strand displacement cascade, and the DNA walkers were driven to move along the track by adding target let-7a [17]. Chen et al. utilized nicking endonucleases Nt.AlwI as the driving force to construct a DNA walking machine and modified electrochemiluminescence labels to achieve sensitive detection of target DNA by signal changes [18]. Therefore, design of an effective and rapid DNA walker efficiently combined with electrochemiluminescence biosensor has huge potential.

For the construction of efficient ECL biosensor platform, the use of novel, nontoxic, and stable ECL luminescent materials as electrode materials was indispensable [19]. Nanocomposites have been widely employed in ECL biosensors owing to their fascinating electrical conductivity, outstanding electrocatalytic activities, satisfactory biocompatibility, and large specific surface area [20]. Graphene quantum dots (GQDs), a novel quasi-zero-dimensional material, not only possess excellent properties of graphene, but also exhibit a series of new functions owing to quantum confinement and edge effects [21, 22]. Compared with the conventional ECL materials (organic fluorophores and semiconductor quantum dots), GQDs have the functions of low cost, good solubility, ease of functionalization, and excellent biocompatibility, which has been used to establish ECL sensors [23]. Molybdenum disulfide (MoS_2) is a typical layered transition metal binary compound with Van der Waals force interacting between layers, which has many potential applications on account of its superior electrochemical, mechanical, and optical performance [24–26]. In addition, it has been reported that the combination of other nanomaterials with this layered material would be expected to exhibit fascinating characteristics [27, 28]. Li et al. investigated the GQDs/MoS_2 heterostructure for the first time [29], which explained the interfacial charge transfer process of carbon-based quantum dot materials and two-dimensional materials, providing a new means for the application of new low-dimensional heterojunction materials in biomedical sensing, micro-nanoelectronic devices, and other fields. Since then, MoS_2-GQDs have been applied to photodetectors and electrochemical biosensors [30, 31]. MoS_2-GQDs hybrid nanocomposites can not only be used as carriers of signal molecules, but also increase the interfacial electron transfer, which has the characteristics of remarkable enhanced ECL [32]. Therefore, it is promising to design a sensing platform for DNA assay via the combination of MoS_2 and GQDs.

In this work, an innovative ECL biosensor for quantitative analysis of target DNA was proposed based on the advantages of MoS_2-GQDs composites and the enzyme-assisted recycling DNA walker amplification strategy. Scheme 1 demonstrated the assembly procedure of the biosensor and the principle of electrochemiluminescence for the assay of target DNA. Firstly, MoS_2-GQDs were immobilized onto the glassy carbon electrode (GCE) surface to obtain a sensing interface. After that, the amino-modified hairpin probe (H) was fixed onto the MoS_2-GQDs nanocomposites via CO-NH bond to achieve signal "on" state. In the existence of target, the hairpin of H was opened to form H-target DNA double strand. Subsequently, the target DNA single strand was released from the H-target DNA double stranded to start the next hybridization and cleavage cycle with the aid of exonuclease III (Exo III). Finally, the ferrocene labeled probe (DNA2-Fc-DNA1) was introduced on the GCE to achieve the signal "off" state. Notably, the function of DNA2 was to prevent hairpin probe H from hybridizing with Fc-DNA1 prior to the target recycle

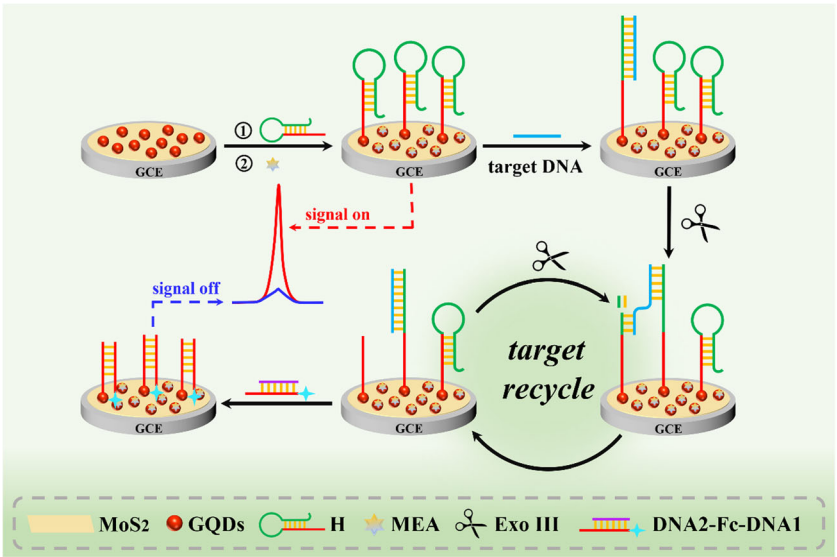

Scheme 1 Fabrication and detection principle of the ECL biosensor platform

process. As expected, the prepared ECL biosensor achieved the sensitive detection of target DNA.

Experimental section

Materials and apparatus

The materials and apparatus have been described in the Electronic Supplementary Material (ESM).

Synthesis of MoS_2

The MoS_2 was synthesized according to the previous literature [33]. Briefly, 1.2 g $H_{24}Mo_7N_6O_{24}{\cdot}4H_2O$ and 2.3 g thiourea were dissolved in 35 mL of ultrapure water under stirring, and the homogeneous solution was formed by sonication. Subsequently, the above mixture was placed into Teflon-lined stainless-steel autoclave and reacted at 220 °C for 4 h. After centrifugation and washing, the black precipitate was collected and frozen overnight in refrigerator. Finally, the target product was obtained by vacuum freeze-drying for 20 h.

Fabrication of biosensor

First, 6 mg MoS_2 and 4 mg GQDs were dissolved in the mixed solution of 10 mL N,N-dimethylformamide (DMF) and H_2O (V(DMF)/V(H_2O) = 1:1) and ultrasonicated in ultrapure water for 3 h to form a uniform suspension. Afterwards, 15 μL of 0.2 M 1-(3-dimethylaminopropyl)-3-ethylcarbodiimide hydrochloride (EDC) and 15 μL of 0.05 M N-hydroxy succinimide (NHS) were mixed with 100 μL of the prepared MoS_2-GQDs solution for 30 min, in which the carboxyl group of GQDs was activated. Before modification, the bare electrode was scoured by 0.3 and 0.05 μm alumina powder, and the mirror-like surface was obtained after cleaning. After that, 10 μL MoS_2-GQDs suspension solution was dropped on a cleaned electrode surface and dried at room temperature. Subsequently, the MoS_2-GQDs/GCE was connected with the H probe (100 μL, 0.5 μM) at 4 °C for 4 h through the CO-NH bond. After rinsed with 0.1 M phosphate buffer (PB, pH 7.4), 10 μL of monoethanolamine (MEA, 10 mM) was coated on the above-modified GCE and reacted for 1 h to block remaining nonspecific binding sites. Eventually, the MEA/H/MoS_2-GQDs/GCE was cleaned with PB (0.1 M, pH 7.4) and preserved at 4 °C for subsequent experiments.

ECL measurement procedure

Scheme 1 presented the running process of DNA walker. Firstly, H/MoS_2-GQDs/GCE was immersed in 10 μL diverse concentrations of target DNA solution at 37 °C for 1 h. After rinsing, the modified GCE was incubated with 10 μL of 0.4 U μL^{-1} Exo III solution for 50 min to digest the H-target DNA double strand and release target DNA, thus realizing the target recycle of DNA walker. Subsequently, the 100 μL mixed solution containing DNA2 (0.5 μM) and Fc-DNA1 (0.5 μM) were denatured at 95 °C for 10 min, and then cooled down at room temperature to form the DNA2-Fc-DNA1 probe. Ultimately, the 10 μL of DNA2-Fc-DNA1 solution was reacted with the prepared GCE for 1 h at 37 °C to hybridize with the remaining part of hairpin H and fixed on the modified GCE surface. The modified electrode was cleaned with PB (0.1 M, pH 7.4) to remove the physically adsorptive species.

The ECL intensity was investigated by the MPI-E multifunctional ECL analytical system in 0.1 M PB (pH 7.4) containing 30 mM $K_2S_2O_8$ and 0.1 M KCl, with potential scanning from −1.95 to 0 V, the scanning rate was 100 mV/s, and the voltage of the photomultiplier tube (PMT) was set at 800 V.

Results and discussion

Choice of materials

Luminescent materials are one of the important factors affecting the performance of ECL biosensors. It is very important to use novel, nontoxic, and stable ECL luminescent materials to build a sensing platform. Compared with other ECL materials such as gold cluster and carbon dots, GQDs have the advantages of low cost, easy functionalization, and excellent biocompatibility. In addition, GQDs have abundant carboxyl groups to provide active sites, and showed strong ECL activity with $K_2S_2O_8$ as coreactant. Combining nanomaterials with GQDs has unexpected properties. MoS_2 has become the most suitable material because of its unique two-dimensional (2D) layered structure, good conductivity, and catalytic activity. The MoS_2 accelerated the electron transport in the ECL process of GQDs, causing a significant enhancement in the ECL signal strength. Therefore, MoS_2-GQDs nanocomposites were chosen to build the sensing platform for DNA detection.

Characterizations of nanomaterials

The surface morphology of related nanomaterials was characterized by scanning electron microscopy (SEM), transmission electron microscopy (TEM), and atomic force microscopy (AFM). The SEM images (Fig. 1a) verified the morphology feature of the synthesized MoS_2, showing the shape of the nanosheets with the size of 200–300 nm. The corresponding TEM images (Fig. 1b) further validated the lamellar construction of the MoS_2 nanosheet. The MoS_2 nanosheets exhibited filmy and folded with suitable support structure. The elements in MoS_2 nanosheets were further confirmed by the energy-

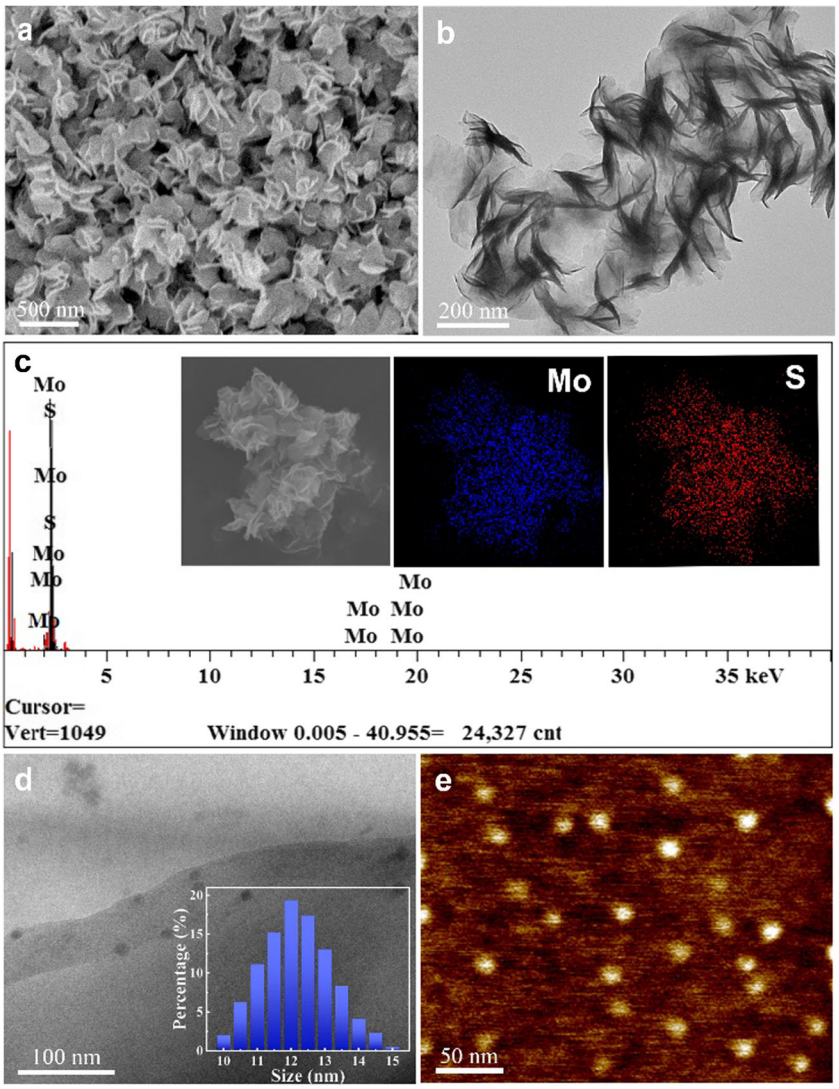

Fig. 1 **a** SEM and **b** TEM images of MoS2. **c** EDX analysis of MoS2. Inset: SEM image and EDX element mapping of MoS2. **d** HRTEM images of GQDs. Inset: the size distribution of GQDs. **e** AFM images of GQDs

dispersive X-ray spectroscopy (EDX) (Fig. 1c), and the contents of Mo and S were 66.89 and 33.11 wt.%, respectively (Table S2). Furthermore, the element distribution in MoS_2 nanosheets was analyzed by elemental mapping of field-emission SEM (FE-SEM). As expected, Mo and S were observed uniformly distributed in the sample (inset of Fig. 1c). The high-resolution TEM (HRTEM) (Fig. 1d) and AFM (Fig. 1e) images showed that the GQDs were uniformly spherical. As depicted in the inset of Fig. 1d, the lateral dimensions of GQDs were in the range of 10–15 nm and the average diameter was 12 nm (n = 65). The SEM characterization of electrode surface was shown in ESM Fig. S1.

Optical properties of the GQDs were investigated by Raman and photoluminescence (PL) spectra. As exhibited in Fig. 2a, the Raman spectrum of GQDs clearly revealed two prominent Raman features G and D bands at 1592 cm^{-1} and 1363 cm^{-1}, respectively. Afterward, the PL spectra of GQDs were investigated at different excitation wavelengths. As shown in Fig. 2b, upon the excitation wavelength of 380 nm, the GQDs have a strong peak at 434 nm. In addition, the GQDs exhibited PL characteristics of dependent excitation. With the increase of excitation wavelength, the PL emission peak showed red shift, which might be caused by different emission sites of GQDs. Moreover, the X-ray photoelectron spectroscopy (XPS) was used for elemental analysis of the synthesized MoS_2-GQDs. The results illustrated that the prepared MoS_2-GQDs incorporated C, Mo, and S elements (Fig. 2c). As shown in Fig. 2d, the XPS peaks in Mo 3d were primary located at 229.5 and 232.7 eV, which were referred to Mo 3d5/2 and Mo 3d3/2 orbitals, respectively. Apparently, the S 2p peak in Fig. 2e expressed two peaks at 162.3 and 163.5 eV, which could be attributed 2p3/2 and 2p1/2 of S derived from the Mo-S bonding in MoS_2. The characteristic peak of C 1S orbitals was shown in Fig. 2f. On the basis of the elemental analysis, the formation of MoS_2-GQDs was further confirmed.

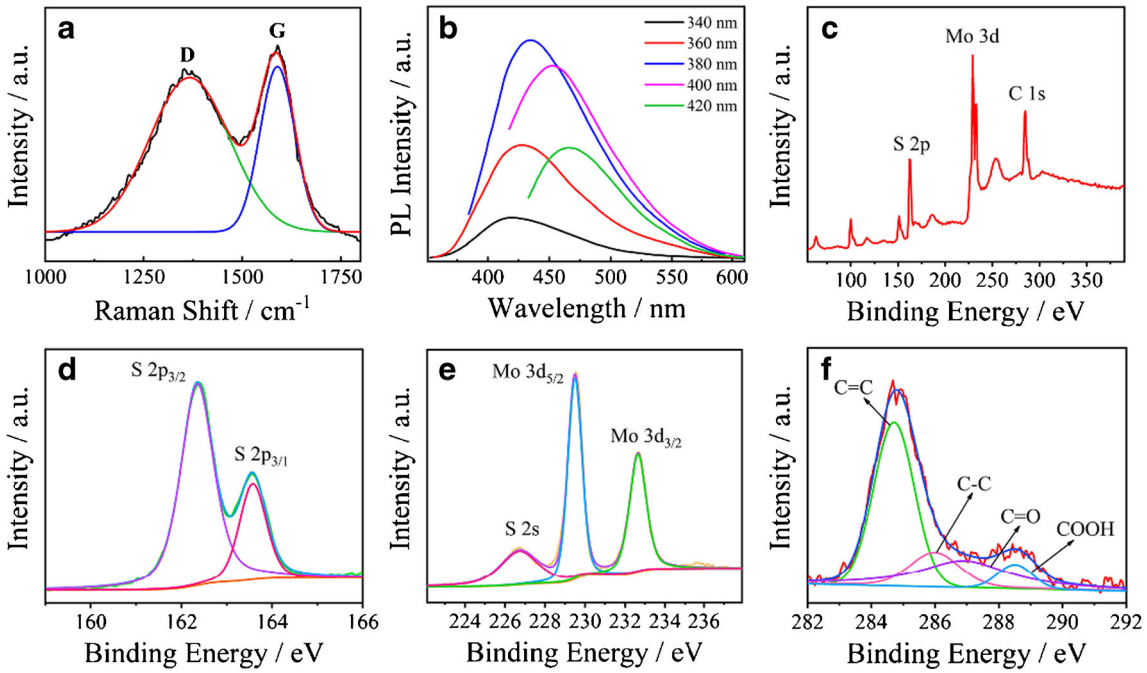

Fig. 2 **a** Raman spectra of GQDs. **b** PL spectra of GQDs acquired using different excitation wavelengths. **c** XPS survey spectra of MoS2-GQDs hybrid nanocomposite. XPS spectra of the **d** Mo 3d, **e** S 2p, and **f** C 1 s region of MoS2-GQDs

ECL performance of MoS_2-GQDs hybrid nanocomposite

To confirm the luminescent properties of the prepared materials, we compared the ECL signals of various modified GCE under the same conditions. As depicted in Fig. 3a, there was no significant differences of ECL responses between bare GCE (curve a) and MoS_2 modified GCE (curve b), indicating that there was no ECL enhancing effect in MoS_2 alone. The ECL strength of GQDs modified GCE was relatively high, which was caused by the ECL performance of GQDs. More impressive, owing to the assistance of MoS_2, ECL signal of MoS_2-GQDs modified GCE (curve c) was greatly enhanced, which was ~8, ~105, and ~243 folds higher than that of GQDs/GCE, MoS_2/GCE, and bare GCE, respectively. Such preliminary consequence affirmed that the MoS_2-GQDs significantly enhanced the ECL process of GQDs. Therefore, the MoS_2-GQDs were selected to prepare the ECL biosensor.

Moreover, the ratio of MoS_2-GQDs has great influence on ECL performance. As displayed in Fig. 3b, with the increase of MoS_2:GQDs mass ratio, the ECL signal gradually added and attained the maximum at the ratio of 6:4 in MoS_2:GQDs. Then, the ECL signal decreased gradually, which indicated that the ECL performance of GQDs could be improved by appropriate doping of MoS_2. Therefore, we chose to prepare MoS_2-GQDs at a mass ratio of 6:4.

Electrochemiluminescence characterization of the biosensor

According to previous literature, cyclic voltammetry (CV) and electrochemical impedance spectroscopy (EIS) have been used for the characterization of modified GCE [34]. Therefore, we used

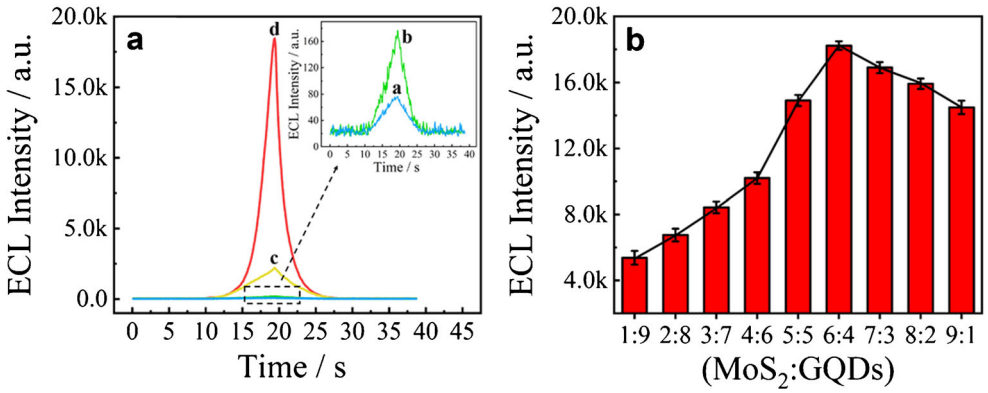

Fig. 3 **a** ECL response curves of (a) bare GCE, (b) MoS2/GCE, (c) GQDs/GCE, and (d) MoS2-GQDs/GCE in 0.1 M PB (pH 7.4) containing 30 mM K2S2O8. **b** The effect of MoS2/GQDs mass ratio on the ECL intensity (error bars show S.D., $n = 3$)

these techniques to analyze the assembly process of biosensors step by step. As exhibited in Fig. 4a, the bare electrode showed the redox peak of $[Fe(CN)_6]^{3-/4-}$ (curve a). After the electrode was modified with MoS_2-GQDs, the peak current increased on account of the acceleration of electron transfer of MoS_2-GQDs, indicating that the nanocomposites were successfully immobilized on the electrode (curve b). When H was incubated onto the MoS_2-GQDs/GCE, the peak current obviously decreased owing to the electron repelling between the negative charges of DNA backbones and electroactive $[Fe(CN)_6]^{3-/4-}$ (curve c). After blocking with the MEA, the current response dropped further (curve d). Then, on the account of introducing more negative charges on GCE, the addition of target DNA led to the decrease of signal response (curve e). However, after treatment of Exo III, the CV current response increased, which was attributed to the continuous cracking process of double strand and the formation of H short products (curve f). After being immersed in the solution of DNA2-Fc-DNA1, the remainder of H could capture Fc-DNA1 through hybridization; thus, the CV peak decreased significantly (curve g). Moreover, the EIS results of ECL biosensor demonstrated in Fig. 4b also confirmed the successful modification of the electrode. In contrast with the bare GCE (curve a), the MoS_2-GQDs/GCE charge-transfer resistance decreased (curve b). However, the continuous introduction of negatively charged H (curve c) and non-conductive MEA (curve d) would cause the charge transfer resistance (R_{et}) to continuously increase. And after incubation with the target DNA, the R_{et} further increased (curve e). Then, the Exo III was added, the R_{et} decreased remarkably (curve f). Finally, when the DNA2-Fc-DNA1 was fixed on the electrode surface, the semicircle diameter raised markedly (curve g). The combined results of CV and EIS characterization measurements confirmed successful fabrication of the proposed ECL biosensor.

Optimization of method

The following parameters were optimized: (a) concentration of GQDs; (b) concentration of Exo III; (c) cleaving time of Exo III; (d) concentration of DNA2-Fc-DNA1;(e) hybridization time between H and DNA2-Fc-DNA1. Respective texts and figures on optimizations were given in the ESM. In short, the following experimental conditions were found to give best results: (a) best concentration of GQDs: 0.4 mg mL^{-1}; (b) best concentration of Exo III: 0.4 U μL^{-1}; (c) best cleaving time of Exo III: 50 min; (d) best concentration of DNA2-Fc-DNA1: 0.5 μM; and (e) best hybridization time between H and DNA2-Fc-DNA1: 60 min.

Performance of the proposed biosensor

To further investigate the analysis properties of the prepared biosensor, the target DNA concentration was determined using the "on-off" mode. As exhibited in Fig. 5a, under the optimal experimental conditions, the ECL signal gradually decreased with the increasing of the target DNA concentration (curves a to h). Obviously, there was a significant linear relationship between the ECL intensity and the logarithmic values of the target DNA concentration from 1 nM to 100 aM, and the regression equation was $I = -14{,}205.75 - 1871.23 \log c$ ($R^2 = 0.9973$, inset of Fig. 5a). With a signal-to-noise ratio (S/N) of 3, the limit of detection (LOD) was evaluated to be 25.1 aM (the calculation process of LOD was shown in ESM). Therefore, the prepared biosensor for the assay of target DNA owned high sensitivity and low detective limit. (The comparison with other DNA detection schemes was shown in ESM Table S3.)

It was known that selectivity was a critical factor in assessing the biosensor. Therefore, the specificity was evaluated by introducing three-base mismatched DNA (T1), non-terminal one-base mismatched DNA (T2), 5′ end one-base mismatched DNA (T3), 3′ end one-base mismatched DNA (T4), target DNA, and mixed sample as the contrast objects. As exhibited in Fig. 5b, the ECL signal of T1 (1 nM) was alike to that of blank (absence of target DNA), indicating that there was no quenching reaction. While the signal intensity of the

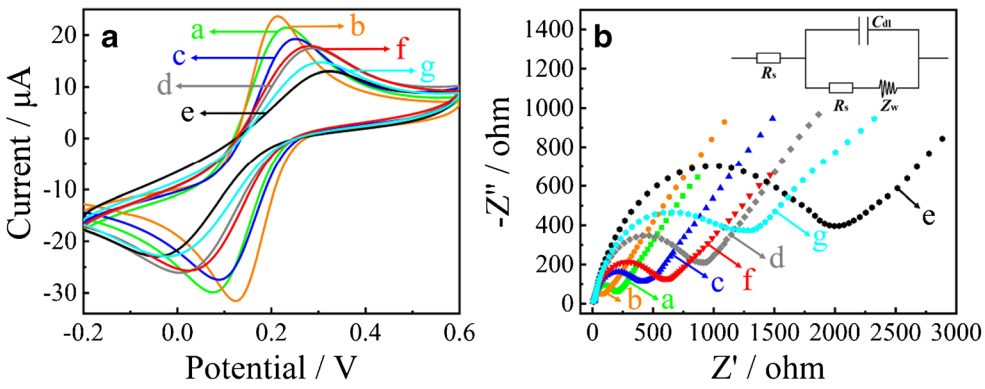

Fig. 4 **a** CV curves and **b** EIS plots of different modified electrodes in PB (0.1 M, pH 7.4) including 5.0 mM [Fe(CN)6]3−/4−: (a) bare GCE; (b) MoS2-GQDs/GCE; (c) H/MoS2-GQDs/GCE; (d) MEA/H/MoS2-GQDs/GCE; (e) target DNA/MEA/H/MoS2-GQDs/GCE; (f) Exo III/target DNA/MEA/H/MoS2-GQDs/GCE; (g) DNA2-Fc-DNA1/Exo III/target DNA/MEA/H/MoS2-GQDs/GCE. Inset of figure b: the equivalent circuit with model impedance data of EIS responses

T2 (1 nM) was relatively reduced. Significantly, when the biosensor reacted with target DNA, its ECL signal decreased greatly. Furthermore, the determination results of T3 (1 nM) and T4 (1 nM) showed that the ECL signal did not decrease significantly when there was single base mismatched at the 5′ end. Nevertheless, when the single base mismatched happened to the 3′ end, the ECL intensity was not apparently different from that of the target DNA. Therefore, in order to avoid the influences of the above situation on the detection results of target DNA, the five bases (TAACT) of target DNA 3′ end were not complemented to H, which were not participated in hybridization process. Consequently, the above interference signals were negligible. After mixing the T1 (1 nM), T2 (1 nM), T3 (1 nM), and T4 (1 nM) with the target DNA (1 nM), the ECL response showed a great ECL decrease, for which there was no remarkable difference from that of 1 nM target DNA only. The consequences proved that the biosensor performed high specificity.

Moreover, sustained and stable ECL signals were important for target DNA assay. As indicated from Fig. 5c, the ECL intensity of electrode incubated with 100 pM of target DNA was measured in 24 cycles of consecutive cyclic potential scanning. It could be revealed from the results that the obtained biosensor possessed excellent detection effect on target DNA, and the relative standard deviation (RSD) was 1.39%.

Furthermore, the reproducibility of the biosensor was equally vital for target DNA determination. Under identical experimental conditions, five parallel intra-assays and inter-assays were carried out to detect 100 pM of target DNA, and the corresponding RSD was 2.66% and 4.82%, respectively (Fig. 5d). Therefore, the detection method had acceptable reproducibility and precision.

In addition, the anti-interference capability of the ECL biosensor was studied using 10% normal human serum as the simulated matrix, and the corresponding texts and figures were given in ESM. The results showed that the ECL signal has good consistency between complex serum matrices and the PB (0.1 M, pH 7.4), reflecting that the proposed biosensor features an acceptable anti-interference capability.

Real sample analysis in human serum

To evaluate the application potential of the designed ECL biosensor in real sample analysis, three serum samples containing target DNA provided by Shandong Tumor Hospital were tested. The detection results were compared with the reference values, and Table S4 showed an acceptable consistency, with a relative deviation of less than 4.08%. Furthermore, the accuracy of the biosensor was further evaluated by standard addition method (ESM Table S4). Different concentrations (1, 10, and 100 fM) of target DNA standards were added into the corresponding initial human serum samples. The recoveries were 93.0%, 96.7%, and 105.3%, respectively, reflecting that the proposed ECL biosensor has more effective and reliable application prospect in clinic analysis.

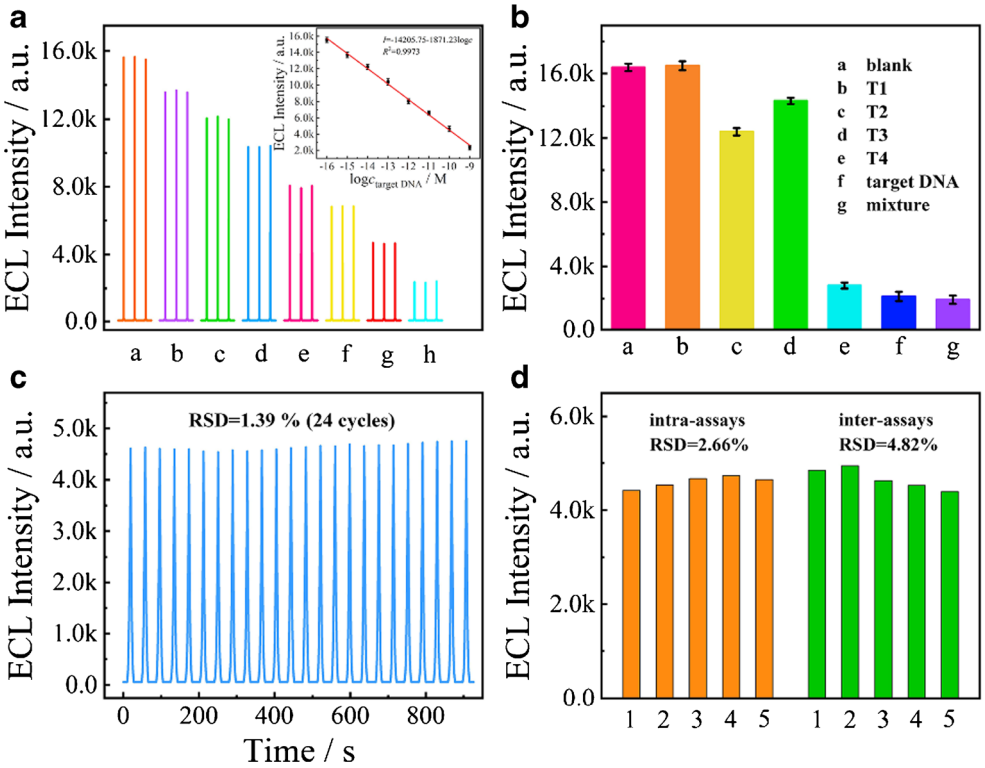

Fig. 5 **a** The ECL response curves of the biosensors with various concentrations of target DNA (a-h: 100 aM-1 nM) in 0.1 M PB (pH 7.4) containing 30 mM K2S2O8. Inset: Linear calibration between the ECL intensity and the logarithm of target DNA concentration. Scanning potential range, −1.95-0 V; scanning rate, 100 mV/s. Error bars show S.D., $n = 3$. **b** Specificity of the ECL biosensor with different DNA sequences (1 nM). Error bars, S.D., $n = 3$. **c** Stability of the biosensor under continuous cyclic potential scan for 24 cycles (100 pM target DNA). **d** Reproducibility of the biosensor in five parallel intra-assays and inter-assays with target DNA concentration of 100 pM

Conclusion

An innovative "on-off" signal switch electrochemiluminescence biosensor based on the excellent luminescent properties of MoS_2-GQDs and enzyme-assisted recycling DNA walker amplification strategy was prepared for sensitive assay of target DNA. The proposed strategy owned various advantages: First, the two-dimensional nanosheet structure of MoS_2 effectively supported the abundant quantum dots and provided more active sites for DNA strands. Second, the prepared nanocomposite (MoS_2-GQDs) accelerated the electron transport in the ECL process and significantly enhanced ECL signal strength. Third, on the basis of enzyme-assisted recycling, DNA walking system strategy realized the further amplification of ECL signal. Further, the developed DNA walker signal amplification ECL biosensor possesses high sensitivity and selectivity for the specific DNA sequence test, which could be applied to clinical analysis and biomedical research.

Supplementary Information The online version contains supplementary material available at https://doi.org/10.1007/s00604-021-04962-3.

Funding This work was supported by the National Natural Science Foundation of China (21775055, 22074053, 21874055); Excellent Youth Innovation Team in Universities of Shandong (2019KJC016); The Project of "20 items of University" of Jinan (2020GXRC047, 2018GXRC001); the Taishan Scholars program and Case-by-Case Project for Top Outstanding Talents of Jinan.

Declarations

Conflict of interest The authors declare no competing financial interests.

References

1. Wang L, Wen Y, Yang X, Xu L, Liang W, Zhu Y, Wang L, Li Y, Li Y, Ding M, Ren S, Yang Z, Lv M, Zhang J, Ma K, Liu G (2019) Ultrasensitive electrochemical DNA biosensor based on a label-free assembling strategy using a triblock polyA DNA probe. Anal Chem 91(24):16002–16009. https://doi.org/10.1021/acs.analchem.9b04757
2. Ding W, Song C, Li T, Ma H, Yao Y, Yao C (2019) TiO_2 nanowires as an effective sensing platform for rapid fluorescence detection of single-stranded DNA and double-stranded DNA. Talanta 199:442–448. https://doi.org/10.1016/j.talanta.2019.02.002
3. Han Y, An F, Liu J, Kong J, Zhang X (2020) Highly sensitive determination of DNA via a new type of electrochemical zirconium signaling probe. New J Chem 44(47):20770–20775. https://doi.org/10.1039/d0nj04405a
4. Dutta S, Dutta Chowdhury A, Biswas S, Park EY, Agnihotri N, De A, De S (2018) Development of an effective electrochemical platform for highly sensitive DNA detection using MoS_2- polyaniline nanocomposites. Biochem Eng J 140:130–139. https://doi.org/10.1016/j.bej.2018.09.016
5. Chen J, Qiu H, Zhang M, Gu T, Shao S, Huang Y, Zhao S (2015) Hairpin assembly-triggered cyclic activation of a DNA machine for label-free and ultrasensitive chemiluminescence detection of DNA. Biosens Bioelectron 68:550–555. https://doi.org/10.1016/j.bios.2015.01.054
6. Wu H, Su Y, Jiang J, Liang Y, Zhang C (2020) Ultrasensitive electrochemiluminescence detection of p53 gene by a novel cloth-based microfluidic biosensor with luminol-gold nanoparticles and hybridization chain reaction amplification. J Luminesc 226:117485. https://doi.org/10.1016/j.jlumin.2020.117485
7. Tang H, Chen W, Li D, Duan X, Ding S, Zhao M, Zhang J (2019) Luminol-based ternary electrochemiluminescence nanospheres as signal tags and target-triggered strand displacement reaction as signal amplification for highly sensitive detection of Helicobacter pylori DNA. Sensors Actuators B Chem 293:304–311. https://doi.org/10.1016/j.snb.2019.05.013
8. Wu Z, Luo F, Wen W, Zhang X, Wang S (2019)Enrichment-stowage-cycle strategy for ultrasensitive electrochemiluminescent detection of HIV-DNA with wide dynamic range. Anal Chem 91(19):12238–12245. https://doi.org/10.1021/acs.analchem.9b01969
9. Zhou S, Gou T, Hu J, Wu W, Ding X, Fang W, Hu Z, Mu Y (2019) A highly integrated real-time digital PCR device for accurate DNA quantitative analysis. Biosens Bioelectron 128:151–158. https://doi.org/10.1016/j.bios.2018.12.055
10. Tao C, Yan Y, Xiang H, Zhu D, Cheng W, Ju H, Ding S (2015) A new mode for highly sensitive and specific detection of DNA based on exonuclease III-assisted target recycling amplification and mismatched catalytic hairpin assembly. Chem Commun 51(20):4220–4222. https://doi.org/10.1039/c5cc00385g
11. He Y, Chen D, Li M, Fang L, Yang W, Xu L, Fu F (2014) Rolling circle amplification combined with gold nanoparticles-tag for ultra sensitive and specific quantification of DNA by inductively coupled plasma mass spectrometry. Biosens Bioelectron 58:209–213. https://doi.org/10.1016/j.bios.2014.02.072
12. Li X, Guo J, Zhai Q, Xia J, Yi G (2016) Ultrasensitive electrochemical biosensor for specific detection of DNA based on molecular beacon mediated circular strand displacement polymerization and hyperbranched rolling circle amplification. Anal Chim Acta 934:52–58. https://doi.org/10.1016/j.aca.2016.06.034
13. Jia L, Shi S, Ma R, Jia W, Wang H (2016) Highly sensitive electrochemical biosensor based on nonlinear hybridization chain reaction for DNA detection. Biosens Bioelectron 80:392–397. https://doi.org/10.1016/j.bios.2016.02.007
14. An N, Li K, Zhang Y, Wen T, Liu W, Liu G, Li L, Jin W (2021) A multiplex and regenerable surface plasmon resonance (MR-SPR) biosensor for DNA detection of genetically modified organisms. Talanta 231:122361. https://doi.org/10.1016/j.talanta.2021.122361
15. Pan J, Li F, Cha TG, Chen H, Choi JH (2015) Recent progress on DNA based walkers. Curr Opin Biotechnol 34:56–64. https://doi.org/10.1016/j.copbio.2014.11.017
16. Shin JS, Pierce NA (2004) A synthetic DNA walker for molecular transport. J Am Chem Soc 126(35):10834–10835. https://doi.org/10.1021/ja047543j
17. Wang L, Deng R, Li J (2015) Target-fueled DNA walker for highly selective miRNA detection. Chem Sci 6(12):6777–6782. https://doi.org/10.1039/c5sc02784e
18. Chen Y, Xiang Y, Yuan R, Chai Y (2015) A restriction enzyme-powered autonomous DNA walking machine: its application for a highly sensitive electrochemiluminescence assay of DNA. Nanoscale 7(3):981–986. https://doi.org/10.1039/c4nr05387g
19. Ma C, Cao Y, Gou X, Zhu JJ (2020) Recent progress in electrochemiluminescence sensing and imaging. Anal Chem 92(1):431–454. https://doi.org/10.1021/acs.analchem.9b04947
20. Huang B, Liu XP, Chen JS, Mao CJ, Niu HL, Jin BK (2020) Electrochemiluminescence immunoassay for the prostate-specific antigen by using a CdS/chitosan/g-C_3N_4 nanocomposite.

Mikrochim Acta 187(3):155. https://doi.org/10.1007/s00604-020-4125-y
21. Li M, Wang C, Chen L, Liu D (2019) A novel electrochemiluminescence sensor based on resonance energy transfer system between nitrogen doped graphene quantum dots and boron nitride quantum dots for sensitive detection of folic acid. Anal Chim Acta 1090:57–63. https://doi.org/10.1016/j.aca.2019.09.018
22. Shekari Z, Zare HR, Falahati A (2019) Electrochemical sandwich aptasensor for the carcinoembryonic antigen using graphene quantum dots, gold nanoparticles and nitrogen doped graphene modified electrode and exploiting the peroxidase-mimicking activity of a G-quadruplex DNAzyme. Mikrochim Acta 186(8):530. https://doi.org/10.1007/s00604-019-3572-9
23. Zhang X-L, Li X, Li X-T, Gao Y, Feng F, Yang G-J (2019) Electrochemiluminescence sensor for pentoxifylline detection using Au nanoclusters@graphene quantum dots as an amplified electrochemiluminescence luminophore. Sensors Actuators B Chem 282:927–935. https://doi.org/10.1016/j.snb.2018.11.113
24. Wang H, Yuan H, Sae Hong S, Li Y, Cui Y (2015) Physical and chemical tuning of two-dimensional transition metal dichalcogenides. Chem Soc Rev 44(9):2664–2680. https://doi.org/10.1039/c4cs00287c
25. Song Y, Qiao J, Li W, Ma C, Chen S, Li H, Hong C (2020) Bimetallic PtCu nanoparticles supported on molybdenum disulfide-functionalized graphitic carbon nitride for the detection of carcinoembryonic antigen. Mikrochim Acta 187(9):538. https://doi.org/10.1007/s00604-020-04498-y
26. Lin Y, Chen X, Lin Y, Zhou Q, Tang D (2015) Non-enzymatic sensing of hydrogen peroxide using a glassy carbon electrode modified with a nanocomposite made from carbon nanotubes and molybdenum disulfide. Microchim Acta 182(9–10):1803–1809. https://doi.org/10.1007/s00604-015-1517-5
27. Ma X, Du C, Zhang J, Shang M, Song W (2019) A system composed of vanadium(IV) disulfide quantum dots and molybdenum(IV) disulfide nanosheets for use in an aptamer-based fluorometric tetracycline assay. Mikrochim Acta 186(12):837. https://doi.org/10.1007/s00604-019-3983-7
28. Govindasamy M, Chen S-M, Mani V, Akilarasan M, Kogularasu S, Subramani B (2016) Nanocomposites composed of layered molybdenum disulfide and graphene for highly sensitive amperometric determination of methyl parathion. Microchim Acta 184(3):725–733. https://doi.org/10.1007/s00604-016-2062-6
29. Li Z, Ye R, Feng R, Kang Y, Zhu X, Tour JM, Fang Z (2015) Graphene quantum dots doping of MoS_2 monolayers. Adv Mater 27(35):5235–5240. https://doi.org/10.1002/adma.201501888
30. Vasilescu I, Eremia SA, Kusko M, Radoi A, Vasile E, Radu GL (2016) Molybdenum disulphide and graphene quantum dots as electrode modifiers for laccase biosensor. Biosens Bioelectron 75:232–237. https://doi.org/10.1016/j.bios.2015.08.051
31. Chen C, Qiao H, Lin S, Man Luk C, Liu Y, Xu Z, Song J, Xue Y, Li D, Yuan J, Yu W, Pan C, Ping Lau S, Bao Q (2015) Highly responsive MoS_2 photodetectors enhanced by graphene quantum dots. Sci Rep 5:11830. https://doi.org/10.1038/srep11830
32. Yang Y, Fang G, Wang X, Zhang F, Liu J, Zheng W, Wang S (2017) Electrochemiluminescent graphene quantum dots enhanced by MoS_2 as sensing platform: a novel molecularly imprinted electrochemiluminescence sensor for 2-methyl-4-chlorophenoxyacetic acid assay. Electrochim Acta 228:107–113. https://doi.org/10.1016/j.electacta.2017.01.043
33. Xie J, Zhang H, Li S, Wang R, Sun X, Zhou M, Zhou J, Lou XW, Xie Y (2013) Defect-rich MoS_2 ultrathin nanosheets with additional active edge sites for enhanced electrocatalytic hydrogen evolution. Adv Mater 25(40):5807–5813. https://doi.org/10.1002/adma.201302685
34. Xie S, Dong Y, Yuan Y, Chai Y, Yuan R (2016) Ultrasensitive lipopolysaccharides detection based on doxorubicin conjugated N-(Aminobutyl)-N-(ethylisoluminol) as electrochemiluminescence indicator and self-assembled tetrahedron DNA dendrimers as nanocarriers. Anal Chem 88(10):5218–5224. https://doi.org/10.1021/acs.analchem.6b00276